THE AERODYNAMICS OF BIRD FLIGHT

Progress Report

for Period of

March 1 - September 1, 1975

Principal Investigator

S. E. Widnall

Ali R. Ahmadi

and

Alexander Krynytzky

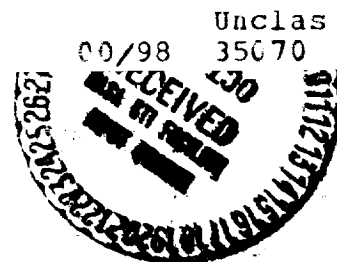Massachusetts Institute of Technology

September 1975

CONTENTS

I. INTRODUCTION

This report is a summary of our theoretical and experimental work during the period of March 1 to September 1, 1975, under NASA Contract NGR 22-009-818 to Langley Research Center.

The aerodynamics of bird flight is rich with many problems of fundamental interest to the fluid mechanician, since the primary reason for the amazing efficiency of birds in flight is probably their highly refined aerodynamics. Examples are optimum configurations and motions, compliant surfaces, porous surfaces, variable geometries, and boundary layer control devices.

Our theoretical research during this period was aimed at studying the aerodynamics of flapping flight. Due to the complexity of the full three-dimensional problem, a two-dimensional flat plate in oscillatory motion of small amplitude was considered first. Most of the analysis of this problem has been completed and a summary is found herein. We expect to complete this analysis soon and then to proceed to the analysis of the more realistic, more challenging and more rewarding problem of a three-dimensional flapping wing. This problem will probably require the use of unsteady lifting surface theory and calculus of variations to optimize the wing configuration and motion.

Experimental work undertaken during this period included the design and specification of a flapping wing model for wind tunnel testing. This model will be capable of pure harmonic flapping of variable amplitude and frequency. Both lift and combined thrust/drag forces will be measured as a function of time. The next steps will be the construction and testing of the model to determine its operating envelope (in the three-dimensional space of flapping amplitude, frequency, and tunnel speed) and to evaluate the accuracy of the force measurements.

II. THEORETICAL WORK

The problem under consideration is to determine, via the use of the momentum theorem, the net streamwise force on a flat plate of zero thickness, placed in a uniform stream, performing small amplitude lateral oscillations. The flow is assumed to be inviscid and incompressible.

2.1 Momentum Theorem

The momentum theorem for a general three-dimensional unsteady motion can readily be formulated in the form (see Fig. 1)

$$\vec{F}_{body} = - \iint_S P\vec{n}dS - \iint_{S+\sigma} \rho\vec{Q}(\vec{Q}\cdot\vec{n}) \, dS - \iiint_V \frac{\partial}{\partial t}(\rho\vec{Q}) \, dV \qquad (1)$$

Making use of the continuity equation and introducing non-dimensional perturbation velocities

$$(S = S_1 + S_2 + S_3)$$

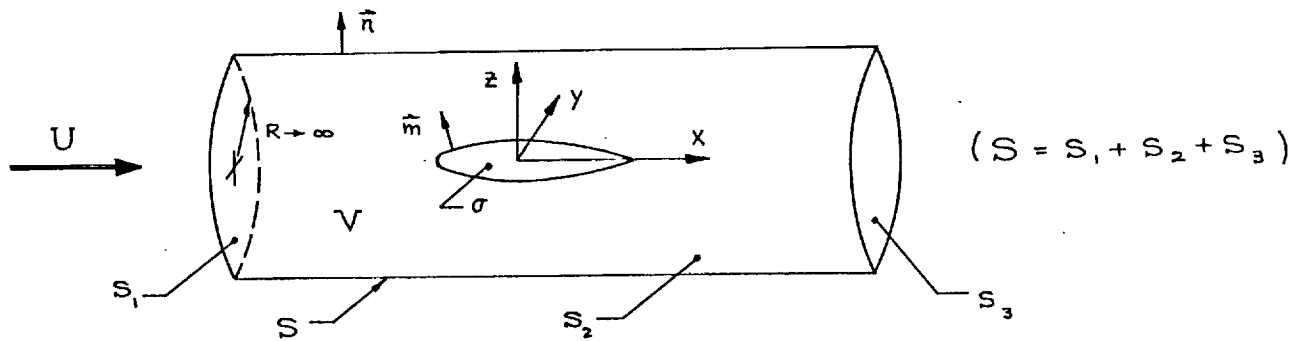Figure 1

$$\vec{Q} = U(\vec{q} + \vec{i}) \qquad (2)$$

Equation (1) becomes

$$\vec{F}_{body} = - \underbrace{\iint_S P\vec{n}dS}_{\vec{A}} - \underbrace{\rho U \iint_S \vec{q}(\vec{Q}\cdot\vec{n}) \, dS}_{\vec{B}} - \underbrace{\rho \iiint_V \frac{\partial}{\partial t}(\vec{Q}) \, dV}_{\vec{C}} - \underbrace{\rho U \iint_\sigma \vec{q}(\vec{Q}\cdot\vec{n}) \, d\sigma}_{\vec{E}} \qquad (3)$$

3

$$= - \vec{A} - \vec{B} - \vec{C} - \vec{E}$$

The x-component of this vector equation is the desired streamwise force (combined thrust and drag).

The x-component of the first term on the right hand side of (3) is simply

$$A_x = \iint\limits_{S_3} (P - P_\infty) \, dS_3$$

Using Bernoulli's equation for unsteady incompressible flow

$$A_x = - \frac{1}{2} \rho U^2 \iint\limits_{S_3} (\frac{2}{U} \phi_t + \phi_x^2 + \phi_y^2 + \phi_z^2 + 2\phi_x) \, dS_3 \qquad (4)$$

The x-component of the second and the third terms are

$$B_x = \rho U^2 \iint\limits_{S_3} (\phi_x + \phi_x^2) \, dS_3 \qquad (5)$$

$$C_x = \rho U \iiint\limits_{V} \frac{\partial}{\partial t} (\phi_x) \, dV \qquad (6)$$

The x-component of the fourth term may be written as

$$E_x = - \rho U \iint\limits_{\sigma} [\vec{q}(\vec{Q} \cdot \vec{m})]_x \, d\sigma \qquad (7)$$

where the subscript 'x' denotes x-component of the vector, and for the sake of convenience, $\vec{n}$ has been replaced by $\vec{m}$ ($\vec{m} = -\vec{n}$). $\vec{m}$ is the outward pointing unit normal at the body surface.

Putting (4) - (7) into (3), we get

4

$$F_x = \frac{1}{2} \rho U^2 \iint_{S_3} [\frac{2}{U} \phi_t + \phi_y^2 + \phi_z^2 - \phi_x^2] \, dS_3 - \rho U \iiint_V \frac{\partial}{\partial t} (\phi_x) \, dV$$

$$+ \rho U \iint_\sigma [\vec{q}(\vec{Q} \cdot \vec{m})]_x \, d\sigma \tag{8}$$

Eq. (8) gives the streamwise force on a three-dimensional body in general unsteady motion. Clearly, the last two integrals in (8) arise as a consequence of the unsteadiness of the motion.

Next, we specialize this general result for the two-dimensional problem under consideration (see Fig. 2).

Figure 2

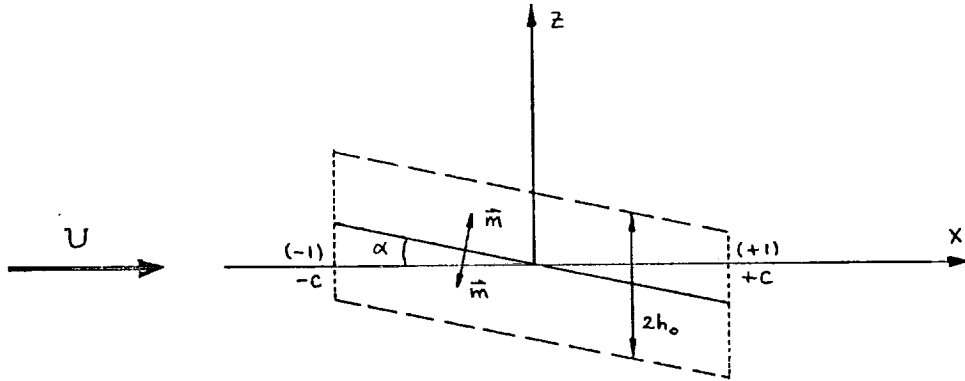For small geometric angle of attack (α), the plate geometry and motion are given by

$$z_{plate}(x, t) = -\alpha x + h_o e^{i \nu t} \tag{9}$$

$$\vec{m} = \pm (\alpha \vec{i} + \vec{k}) \qquad (+, \text{ upper; } -, \text{ lower}) \tag{10}$$

5

The last integral in (8) may be written as the sum of a contribution from upper and lower surfaces and a contribution from the sharp leading and trailing edges of the plate. The former contribution may be written as

$$\rho U^2 \int_{-c}^{c} [\alpha(\phi_{x_u}^2 - \phi_{x_\ell}^2) + (\phi_z + \alpha)(\phi_{x_u} - \phi_{x_\ell})] \, dx \qquad (11)$$

where subscripts 'u' and 'ℓ' denote upper and lower surfaces of the plate. Representing the plate by a vortex sheet ($\phi_{x_u} = - \phi_{x_\ell}$), Eq. (11) reduces to

$$2\rho U^2 \int_{-c}^{c} (\phi_z + \alpha) \, \phi_{x_u} \, dx \qquad (12)$$

where ϕ_z is determined from the boundary condition at the plate,

$$\phi_z = \frac{\partial z}{\partial t} + U \frac{\partial z}{\partial x} \; ; \quad \phi_z = -\alpha - \frac{\nu h_o}{U} \sin(\nu t) \qquad (13)$$

Putting (13) into (12), the contribution from upper and lower surfaces becomes

$$-2\rho U \, \nu h_o \int_{-c}^{c} \sin(\nu t) \, \phi_{x_u} \, dx \qquad (14)$$

With this result, Eq. (8) for two-dimensional case reduces to

$$F_x = \frac{1}{2} \rho U^2 \int_{-\infty}^{\infty} (\frac{2}{U} \phi_t + \phi_z^2 - \phi_x^2) \, dz - \rho U \iint_{-\infty}^{\infty} \frac{\partial}{\partial t} (\phi_x) \, dx \, dz$$

$$-2\rho U \, \nu h_o \int_{-c}^{c} \sin(\nu t) \, \phi_{x_u} \, dx + \rho U \int_{LE+TE} [\vec{q}(\vec{Q} \cdot \vec{m})]_x \, ds \qquad (15)$$

The first integral is to be carried out over the Trefftz plane and 's' denotes distance along the plate contour.

Averaging (15) over time (one period), and remembering that for oscillatory motion time average of a time derivative is zero, we obtain the average streamwise force experienced by the plate.

$$\bar{F}_x = \frac{1}{2} \rho U^2 \int_{-\infty}^{\infty} (\overline{\phi_z^2} - \overline{\phi_x^2})dz - 2\rho U \, \nu h_0 \int_{-c}^{c} \overline{\sin(\nu t) \, \phi_{x_u}} \, dx$$

$$+ \rho U \int_{LE+TE} \overline{[\vec{q}(\vec{Q} \cdot \vec{m})]_x} \, ds \tag{16}$$

In (16), the first contribution to $\bar{F}_x$ is due to pressure and momentum flux in the Trefftz plane, which is the contribution from the wake; while the second and third contributions are due to momentum exchange at the upper and lower surfaces and leading and trailing edges correspondingly. In the following sections, we proceed to evaluate each of these contributions separately.

2.2 Contribution from Wake

The wake of an airfoil in continuous oscillatory motion consists of a continuous band of vortices. For the two-dimensional case, the wake consists of spanwise vortices only. To determine the perturbation velocities in the Trefftz plane, we assume a flat rigid wake and note that the contributions of bound and starting vortices vanish (assuming the motion has been going on indefinitely).

For inviscid and incompressible flow, the velocity potential satisfies Laplace's equation which together with linear boundary conditions allows us to use superposition to build up the desired solution. The coordinate system is attached to the Trefftz plane and moves with the airfoil, as shown in Fig. 3.
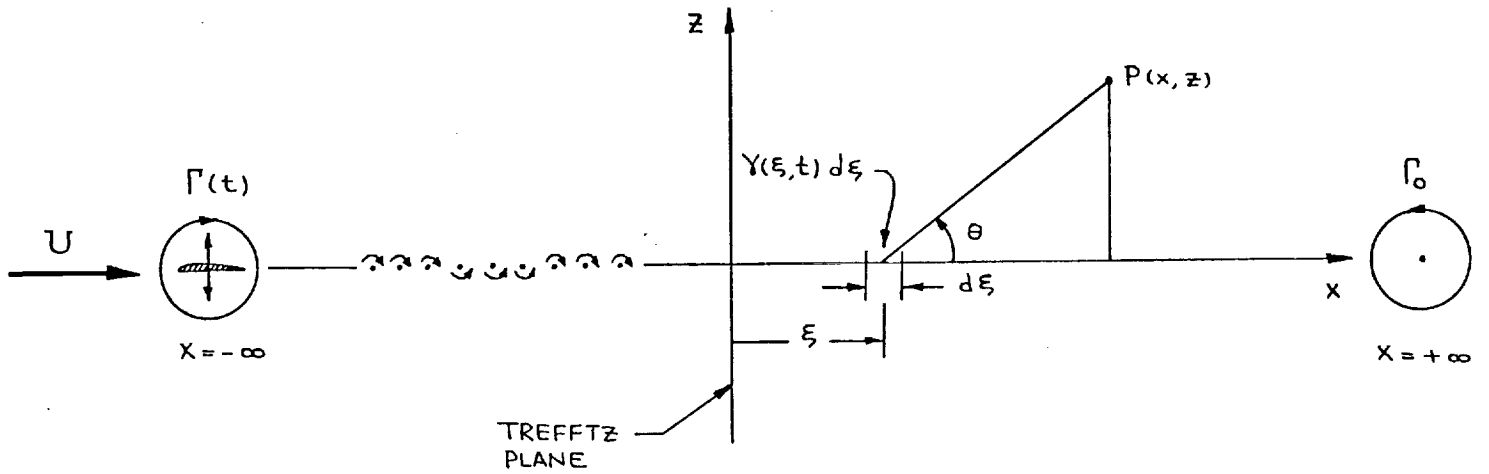
7

Figure 3

The perturbation velocity potential at P(x, z) (for all finite x) due to the doubly infinite wake is readily obtained in the form

$$\phi(x, z, t) = - \frac{1}{2\pi} \int_{-\infty}^{\infty} \gamma(\xi, t) \, \tan^{-1} \left[\frac{z}{x - \xi} \right] d\xi \tag{17}$$

For steady state oscillations that have been going on indefinitely, we may assume

$$\gamma(\xi, t) = g \, e^{i\nu(t - \xi/U)} \tag{18}$$

where 'g' is a constant. Putting (18) into (17) and taking $\frac{\partial}{\partial x}$ and $\frac{\partial}{\partial z}$, we find integral expressions for perturbation velocities at any point with finite x.

$$\phi_x = \frac{gz}{2\pi} \int_{-\infty}^{\infty} e^{i\nu(t - \xi/U)} \frac{d\xi}{(x - \xi)^2 + z^2}$$

$$\phi_z = \frac{-g}{2\pi} \int_{-\infty}^{\infty} e^{i\nu(t - \xi/U)} \frac{(x - \xi) \, d\xi}{(x - \xi)^2 + z^2} \tag{19}$$

8

In the Trefftz plane, $x = 0$, and these reduce to

$$\phi_x = \frac{gz}{2\pi} \int_{-\infty}^{\infty} e^{i\nu(t - \xi/U)} \frac{d\xi}{\xi^2 + z^2} \qquad (20)$$

$$\phi_z = \frac{-g}{2\pi} \int_{-\infty}^{\infty} e^{i\nu(t - \xi/U)} \frac{\xi d\xi}{\xi^2 + z^2} \qquad (21)$$

The real part of (20) can be expressed in terms of the modified Bessel function of the second kind (Ref. 1).

$$\phi_x = \frac{g}{\sqrt{2\pi}} \cos(\nu t) (kz)^{1/2} K_{1/2} (kz) \qquad (z > 0) \qquad (22)$$

Bessel functions of order half an odd integer are expressible in closed form in terms of elementary functions. Hence, Eq. (22) may be written as (ϕ_x has been non-dimensionalized with U)

$$\phi_x = \frac{g}{2U} \cos(\nu t) e^{-kz} \qquad (z > 0) \qquad (23)$$

Since ϕ_x is antisymmetric in z, we may write for all z

$$\phi_x = \pm \frac{g}{2U} \cos(\nu t) e^{-k|z|} \qquad (24)$$

The real part of (21) can be integrated (Ref. 4) to yield

$$\phi_z = \frac{g}{2} \sin(\nu t) e^{-kz} \qquad (z > 0) \qquad (25)$$

Since ϕ_z is symmetric in z, we may write for all z, after non-dimensionalizing ϕ_z with U

$$\phi_z = \frac{g}{2U} \sin(\nu t) e^{-k|z|} \qquad (26)$$

9

Upon squaring (24) and (26) and averaging over one period, we find

$$\overline{\phi_x^2} = \overline{\phi_z^2} = \frac{g^2}{8U^2} \, e^{-2k|z|} \qquad (27)$$

Therefore

$$\int_{-\infty}^{\infty} (\overline{\phi_z^2} - \overline{\phi_x^2}) \, dz = 0 \qquad (28)$$

We conclude that for 2-D small amplitude problem the contribution, to the mean streamwise force, from pressure and momentum flux due to the wake is identically zero.

2.3 Contribution from Plate Surfaces

The second contribution to $\overline{F_x}$ (Eq. 16) comes from momentum exchange at the plate surfaces and is a direct result of the unsteadiness of the motion. To evaluate this contribution, we must determine ϕ_{x_u} (x, t) or equivalently the vorticity distribution, $\gamma(x, t)$, that represents the unsteady motion of the plate.

Due to the linearity of the problem, we may think of $\gamma(x, t)$ as consisting of a quasi-steady part (i.e, neglecting the effect of wake vortices on the plate, say $\gamma_0(x, t)$) and an induced part (i.e., the effect of the wake on the plate, say $\gamma_1(x, t)$).

The quasi-steady vorticity distribution at the plate is the solution of the integral equation of thin airfoil theory (see, e.g., Ref. 2)

$$\gamma(x) = \frac{2\alpha U}{\pi} \sqrt{\frac{1 - x}{1 + x}} \int_{-1}^{1} w(\xi) \sqrt{\frac{1 + \xi}{1 - \xi}} \, \frac{d\xi}{\xi - x} \qquad (29)$$

For flat plate at small α, $w(\xi) = -\alpha_e U$. Putting this into (29) and integrating, we obtain the familiar result

$$\gamma(x) = 2\alpha_e U \sqrt{\frac{1-x}{1+x}} \qquad (30)$$

where α_e is the effective angle of attack and consists of the geometric and induced angles of attack. Assuming small amplitude, moderate frequency oscillations

$$\alpha_i \approx \frac{W}{U}$$
$$\approx -\frac{\nu h_0}{U} \sin(\nu t) \qquad (31)$$

Substituting for α_e in (30), we get the quasi-steady vorticity distribution

$$\gamma_0(x, t) = [2\alpha U - 2\nu h_0 \sin(\nu t)]\sqrt{\frac{1-x}{1+x}} \qquad (32)$$

The induced vorticity at the plate due to one vortex (Γ') in the wake is given by (e.g., see Ref. 5)

$$\gamma(x) = \frac{1}{\pi} \frac{\Gamma'}{\xi - x} \sqrt{\frac{1-x}{1+x}} \sqrt{\frac{\xi+1}{\xi-1}} \qquad (33)$$

Then, for steady state oscillations that have been going on indefinitely, integrating such contributions for a vortex wake extending from $x = c$ to ∞ (or non-dimensional $x = 1$ to ∞), we get the total induced vorticity at the plate,

$$\dot{\gamma}_1(x, t) = \frac{g}{\pi} \int_1^\infty e^{i\nu(t - \xi/U)} \frac{1}{\xi - x} \sqrt{\frac{1-x}{1+x}} \sqrt{\frac{\xi+1}{\xi-1}} \, d\xi \qquad (34)$$

or

$$\gamma_1(x, t) = \frac{g}{\pi} e^{i\nu t} \sqrt{\frac{1-x}{1+x}} \int_1^\infty e^{-ik\xi} \frac{1}{\xi - x} \sqrt{\frac{\xi+1}{\xi-1}} \, d\xi \qquad (35)$$

The 2nd term on the right hand side of (16) may be written as

$$-2\rho U\nu h_0 \int_{-c}^c \overline{\sin(\nu t) \, \phi_{x_u}} \, dx = -2\rho U\nu h_0 \int_{-c}^c \overline{\sin(\nu t) \, [\gamma_0(x, t) + \gamma_1(x, t)]} \, dx \qquad (36)$$

11

Next, we put (32) and (35) into (36) and carry out the integrations. The integrals encountered are handled in the following way.

$$\int_{-c}^{c} \sqrt{\frac{1-x}{1+x}} \, dx = c \int_{-1}^{1} \sqrt{\frac{1-x}{1+x}} \, dx = c\pi \qquad (37)$$

where we have made use of the transformation $x = -\cos\theta$.

$$\frac{1}{\pi} \int_{-c}^{c} \frac{1}{\xi - x} \sqrt{\frac{1-x}{1+x}} \, dx = \frac{1}{\pi} \int_{-1}^{1} \frac{1}{\xi - 1} \sqrt{\frac{1-x}{1+x}} \, dx = \sqrt{\frac{\xi - 1}{\xi + 1}} - 1 \qquad (38)$$

where we have made use of complex variables and Cauchy's integral formula.

$$\int_{1}^{\infty} e^{-ik\xi} \left(1 - \sqrt{\frac{\xi + 1}{\xi - 1}}\right) d\xi = c \frac{e^{-ik}}{ik} - \frac{\pi c}{2} [H_1^{(2)}(k) + i H_0^{(2)}(k)] \qquad (39)$$

the first part of these was done by contour integration and the rest are listed in Ref. 7 . The Hankel functions in (39) may be expressed in terms of Bessel functions J and Y.

Finally, using (37)-(39) in (36), we obtain an expression whose real part upon averaging over time is given by

$$-2\rho U \nu h_o \int_{-c}^{c} \overline{Sin(\nu t) \, \phi_{x_u}} \, dx =$$

$$\rho U k h_o \{\pi \nu h_o - \frac{g}{2k} Cos(k) + \frac{\pi g}{4} [J_o(k) - Y_1(k)]\} \qquad (40)$$

This is the contribution to $\overline{F_x}$ from momentum exchange at the upper and lower surfaces of the plate.

2.4 Contribution from Plate Edges

The 3rd contribution to $\overline{F_x}$ (Eq. 16) comes from momentum exchange at the sharp leading and trailing edges which is a direct result of the

12

unsteadiness of the motion. At the leading edge, velocity becomes infinite and hence we expect a finite contribution to $\overline{F_x}$, while the requirement of smooth flow (Kutta condition) at the trailing edge points to zero contribution. The former requires determining the local flow field which can be done by the method of matched asymptotic expansions. We are currently working on this part of the problem.

III. EXPERIMENTAL WORK

The design and specification of a flapping wing model for the wind tunnel are nearing completion. The design is simple (see Figure 4), consisting of a wing mounted rigidly to one end of a shaft, the other end being driven back and forth by a servomoter. The axis of the shaft is parallel to the free stream air velocity in the wind tunnel. The drive system consists of a one-half horsepower D. C. motor, a rate control loop electronic circuit, a signal generator, and a power supply. It may additionally be required to supplement the rate loop circuit with a position control loop. Flapping amplitude and frequency will be varied simply by changing the frequency and amplitude of the output of the signal generator. The cost of the drive system is approximately as follows:

Servometer with analog rate controller	$654.00
Power-supply	450.00
Position controller	150.00 - 180.00
Signal generator	Available in house
	$1254.00/$1284.00

The motor is rated at 400 oz.-in.continuous torque. The motor-rate controller

response curves are flat out to about 38 Hz where the phase curve starts dropping off. The gain curve stays flat out to about 50 Hz. The maximum flapping frequency presently foreseen is 5-10 Hz. The manufacturer of this system is willing to let us have it on consignment for thirty days so that, if for some reason it was not satisfactory, we could return it.

Other candidates for the drive system were investigated and eliminated during the course of the summer. A bar-slider mechanism driven by constant rotary motion results in a linear oscillatory motion with a significant second harmonic unless the bar is made very long compared to the radius of rotation. A Scotch yoke results in linear oscillatory motion of purely first harmonic nature, but maximum force is required of the Scotch yoke at points in the cycle when the force transmission angles are most unfavorable. The linear oscillatory motion from either of these sources could then be transformed to a rotary oscillatory motion using a rack and pinion. Complexity in design is added by the requirement that the flapping amplitude and frequency be independently variable. Because of the mechanical complexity of such a system, and the uncertainty of its performance once it was built, and because its cost would have been comparable to the servomotor.system, a strictly kinematic solution was rejected in favor of the servomotor system.

The forces on the wing will be measured near its root. A removable strain-gauged flexure will measure bending moment at two different distances from the flapping axis in both the axial and tangential directions relative to the flapping axis (in steady flight, i.e., with no flapping, these correspond to the lift and drag forces). Two bending moment points are required to
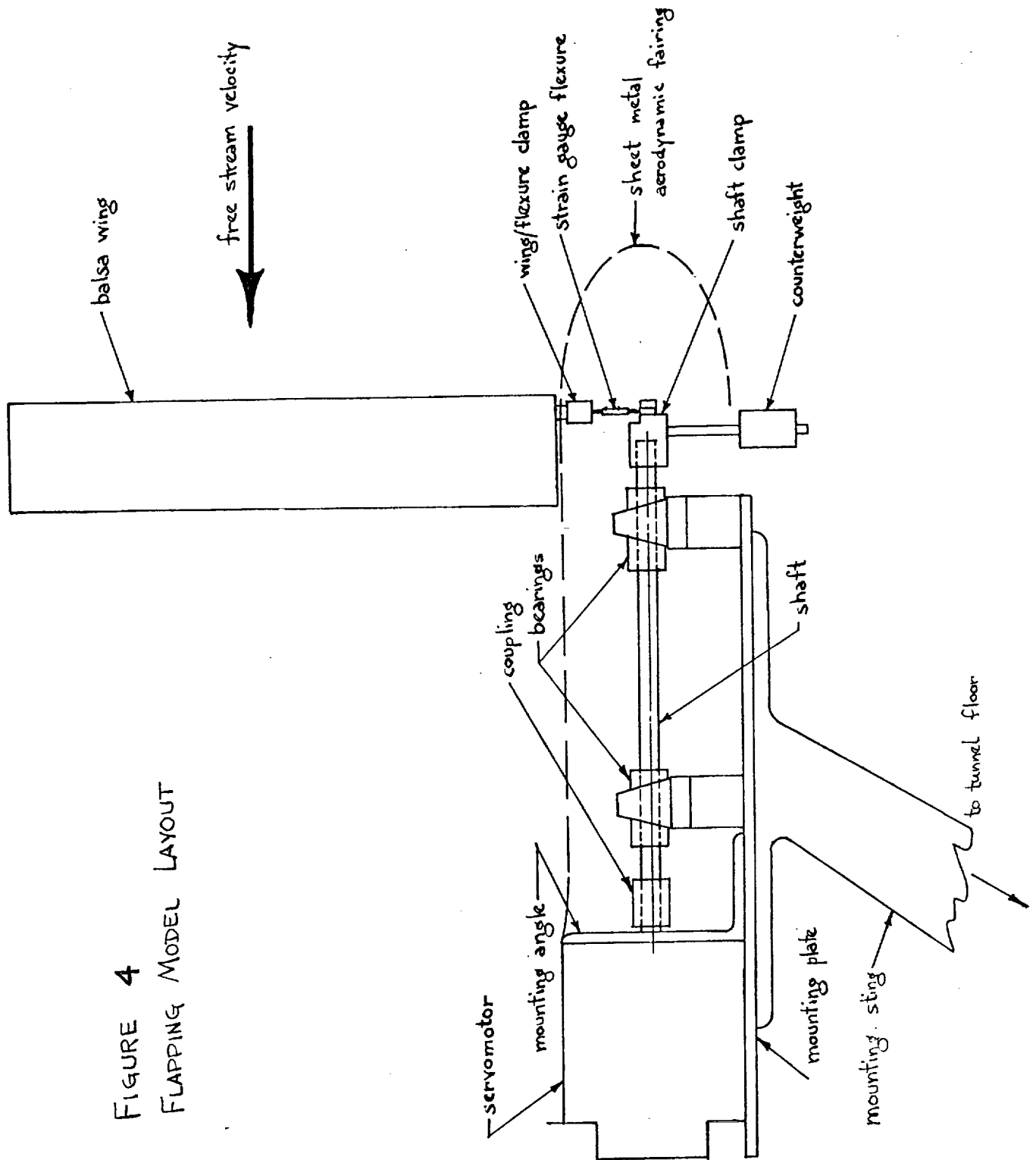
14

characterize the bending moment curve of a beam acted on by a single concentrated force, F_0, at some distance, y_0, from its end (see Figure 5). This curve is, in fact, a straight line. The force, F_0, acting at y_0 is equipollent to the distributed aerodynamic force over the span of the wing and can be determined from the formula

$$F_0 = \frac{M_1 - M_2}{y_1 - y_2}$$

The flexure will have strain gauges on all four faces so it will measure bending moments in two perpendicular planes, resulting in both lift and drag forces. The drag (and thrust) measurements will come directly from the strain gauge data. The measurements for lift, however, will contain the bending moment due to inertial loads generated by the angular acceleration of the wing while flapping, so this component must be calculated and subtracted from the total moment to find the moment due to aerodynamic forces alone.

The wing initially under investigation will be of rectangular plan-form with a three-inch chord and an aspect ratio of about five. The wing section, constant along the span, will be a NACA 0015. The range of flapping amplitude, flapping frequency, initial angle of attack, and free stream velocity will be determined in the course of the first proving tests of the model.

free stream velocity

balsa wing

wing/flexure clamp

strain gauge flexure

sheet metal aerodynamic fairing

shaft clamp

counterweight

coupling

bearings

shaft

servomotor

mounting angle

mounting plate

mounting sting

to tunnel floor

FIGURE 4
FLAPPING MODEL LAYOUT

Equipollent
Aerodynamic Loading
F_0

Distributed Aerodynamic Loading

Aerodynamic Force

O

Y_1 Y_2

Y_0

spanwise coordinate y

Bending Moment in Beam

Y_1 Y_2

O

Y_0

spanwise coordinate y

M_2
M_1
$-F_0 Y_0$

Moment due to concentrated force F_0 acting at Y_0
M_1, M_2 = measured moments at spanwise coordinates y_1 and y_2

$$F_0 = \frac{M_1 - M_2}{Y_1 - Y_2}$$
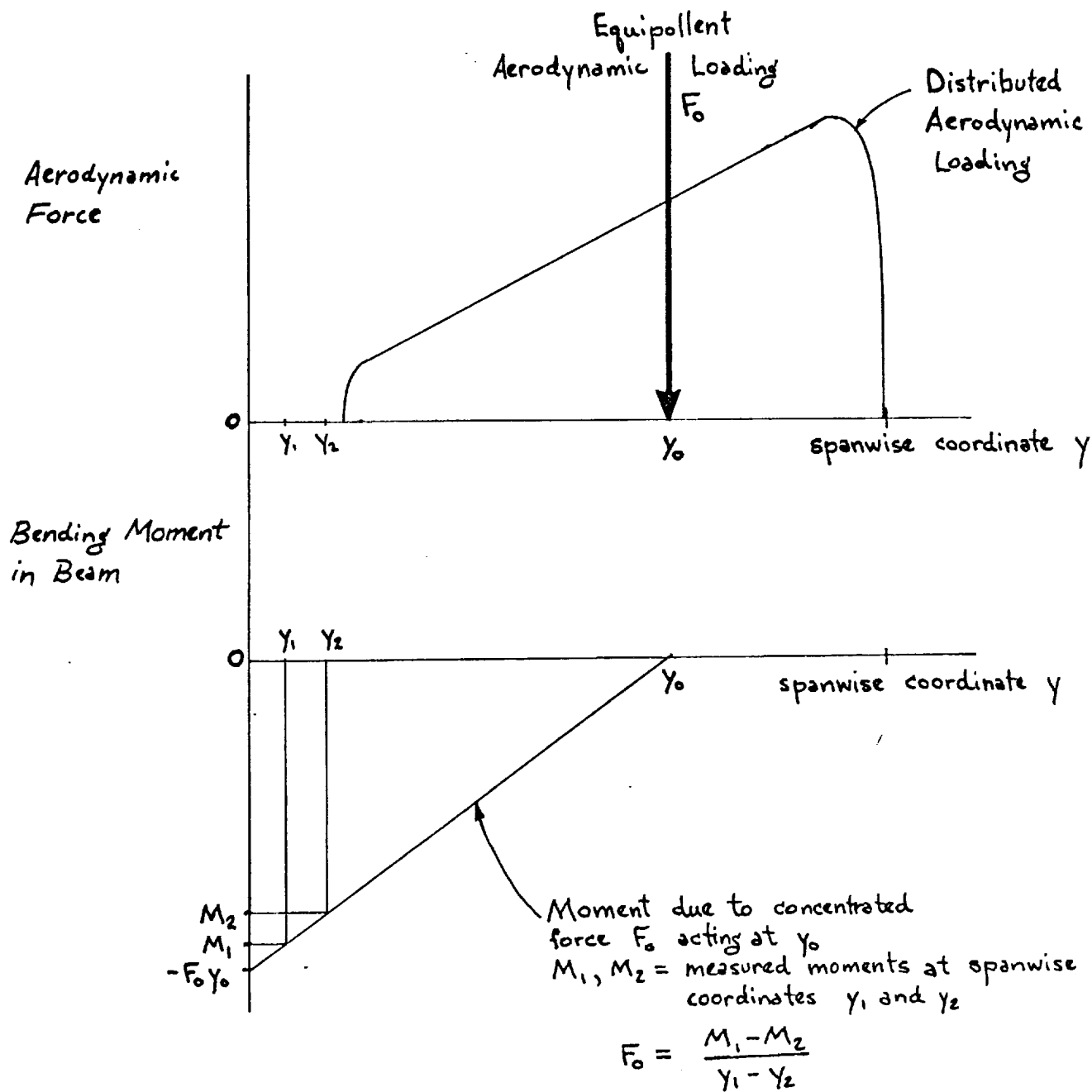
FIGURE 5   MEASUREMENT OF THE AERODYNAMIC FORCE ON A WING

SYMBOLS

c	semi-chord length
$\vec{F}_{body}$	force on body
F_x	streamwise force on body
g	see Eq. (18)
h_o	amplitude of oscillation
$\vec{i}$	unit vector in x-direction
$\vec{j}$	unit vector in y-direction
k	reduced frequency
$\vec{k}$	unit vector in z-direction
$\vec{m}$	outward pointing unit normal at body surface
$\vec{n}$	outward pointing unit normal at fluid control surface
P	pressure
$\vec{q}$	perturbation velocity
$\vec{Q}$	total velocity
s	arc length
S	surface area
t	time
U	free stream velocity
V	volume
w	z-component of perturbation velocity
x	streamwise coordinate[*]
y	spanwise coordinate
z	vertical coordinate[*]
L.E.	leading edge
T.E.	trailing edge

18

α	angle of attack
α_e	effective angle of attack
α_i	induced angle of attack
ρ	density
ϕ	perturbation velocity potential
ξ	distance measured along x-direction[*]
γ	strength of vortex sheet (per unit length)
γ_0	quasi-steady vorticity distribution (per unit length)
γ_1	induced vorticity distribution (per unit length)
Γ	circulation
ν	frequency of oscillation

$(\ )_\ell$	lower
$(\ )_u$	upper
$\overline{(\ )}$	time average

[*] To avoid unnecessary symbolism, x, z and ξ are used as dimensional and non-dimensional (with respect to semi-chord) variables interchangeably; however, this is normally clear from the context. Also, ϕ_x and ϕ_z are used in a similar manner (non-dimensionalized with U).

REFERENCES

1. Abramowitz, M. and Stegun, I. A., 1970, Handbook of Mathematical Functions, U. S. Government Printing Office, Washington, D. C.

2. Ashley, H. and Landahl, M., 1965, Aerodynamics of Wings and Bodies, Addison-Wesley, Reading, Mass.

3. Durand, W. F., editor, 1935, Aerodynamic Theory, Vol. II, Dover Publications, New York.

4. Gradshteyn, I. S. and Ryzhik, I. M., 1965, Tables of Integrals, Series and Products, Academic Press, New York.

5. von Karman, T., and Sears, W. R., Aug. 1938, Airfoil Theory for Nonuniform Motion, J. Aeron. Sci., $\underline{5}$, No. 10, pp. 379-390.

6. Pope, A. and Harper, J. J., 1965, Low Speed Wind Tunnel Testing, John Wiley and Sons, New York.

7. Watson, G. N., 1948, A Treatise on the Theory of Bessel Functions, second edition, The Macmillan Co., London.

8. Yih, C.-S., 1969, Fluid Mechanics, McGraw-Hill Co., New York.